Science of the Total Environment 905 (2023) 167058

Contents lists available at ScienceDirect

Science of the Total Environment

journal homepage: www.elsevier.com/locate/scitotenv

Salinity origin in the coastal aquifer of the Southern Venice lowland

Luigi Alessandrino [a], Mattia Gaiolini [b], Francisco Aldo Cellone [c,d], Nicolò Colombani [b,*], Micòl Mastrocicco [a], Marta Cosma [c], Cristina Da Lio [c], Sandra Donnici [c], Luigi Tosi [c]

[a] DiSTABiF - Department of Environmental, Biological and Pharmaceutical Sciences and Technologies, Campania University "Luigi Vanvitelli", Via Vivaldi 43, 81100 Caserta, Italy
[b] SIMAU - Department of Materials, Environmental Sciences and Urban Planning, Marche Polytechnic University, Via Brecce Bianche 12, 60131 Ancona, Italy
[c] IGG - Institute of Geosciences and Earth Resources, National Research Council, Via G. Gradenigo 6, 35131 Padova, Italy
[d] Centro de Investigaciones del Medio Ambiente, Consejo Nacional de Investigaciones Científicas y Técnicas, Universidad Nacional de La Plata (CIM-UNLP-CONICET), Buenos Aires, Argentina

HIGHLIGHTS

- Salinity origin of coastal aquifer using Cl^- and Br^- in sediment cores
- Concentration profiles combined with depositional facies improved conceptual model
- A salinized site near Venice is used to test the methodology.
- Actual, paleo seawater and evaporites were the main salinization sources.
- Simple salinity measurements may provide misleading results.

GRAPHICAL ABSTRACT

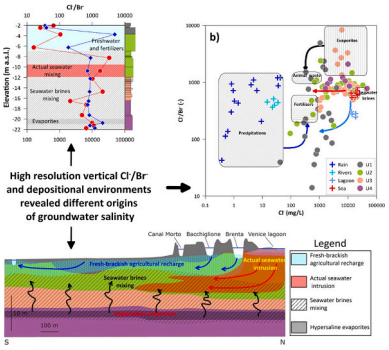

ARTICLE INFO

Editor: Jurgen Mahlknecht

Keywords:
Cl^-/Br^- molar ratio
Sediment porewater
Aquifer salinization
Depositional environments

ABSTRACT

Groundwater salinization can be natural and anthropogenic in origin, although it often results from a combination of both, especially in low-lying coastal regions that are hydraulically controlled. This study proposes a method to assess the origin of salinity using environmental tracers in porewater, like Cl^- and Br^-, combined with depositional facies associations detected in sediment cores. Such integrated approach was tested in a target area south of the Venice Lagoon (Italy), where groundwater salinization is triggered by multiple mechanisms due to the complexity of the hydro-geomorphological environment. Batch tests were performed on sediment core samples from boreholes to quantify major anions and total inorganic N. Cl^- and Br^- porewater concentrations coupled with sedimentary facies association provided insights into the origin of groundwater salinity from a variety of sources, including past and present seawater intrusion, agricultural leaching, and evaporites. The strengths and limitations of the integrated approach are discussed to provide a pathway for improving water resource management and planning measures to prevent groundwater salinization in coastal areas.

* Corresponding author.
E-mail address: n.colombani@univpm.it (N. Colombani).

https://doi.org/10.1016/j.scitotenv.2023.167058
Received 11 June 2023; Received in revised form 10 September 2023; Accepted 11 September 2023
Available online 13 September 2023

1. Introduction

One of the most widespread and alarming phenomena affecting coastal areas is the progressive salinization of freshwater resources (Li et al., 2020). Groundwater salinization occurs at local and regional scales and may have diverse origins (Manivannan and Elango, 2019; Wen et al., 2005). In many cases, it is plausible to assume that seawater intrusion is involved, especially in lowland coastal areas because of small head gradients combined with drainage management. In addition, groundwater depletion where human activities are concentrated (Ashraf et al., 2017; Wu et al., 2013) and climate change, such as sea level rise (Da Lio and Tosi, 2019) and extended periods of below-average rainfall (Mastrocicco and Colombani, 2021), are exacerbating groundwater salinization. However, other natural salt sources or human activities may cause groundwater salinization (Cartwright et al., 2004). Evaporation, evaporite leaching, mobilization of salts stored in the unsaturated zone, infiltration of sewage polluted surface waters, slow-moving saline/salt waters of marine origin, highly mineralized waters from geothermal fields, sea spray, hyper-filtration from aquitards, and agricultural practices are the most significant salt sources/processes globally recognized (Barbecot et al., 2000; Li et al., 2020). Paleo-seawater is also common in coastal plains, both in confined aquifers (Barbecot et al., 2000; Montety et al., 2008) and, at least at patches, in shallow Holocene aquifers (Caschetto et al., 2016; Giambastiani et al., 2021; Kuang et al., 2015; Tran et al., 2012).

For cost-effective management of water resources, it is important to understand the mechanisms that control the exchange of fresh and salt waters, including the vertical variability of groundwater salinity, to calculate the amount and the direction of saline groundwater seepage in lowland coastal areas (de Louw et al., 2010). To monitor the variability of the saltwater-freshwater interface in unconfined aquifers, the profiling of electrical conductivity (EC) recorded using data loggers in fully screened wells is a widespread practice. Nevertheless, this technique has some drawbacks due to intraborehole mixing processes that could alter the saltwater-freshwater interface and redox gradients (Mastrocicco et al., 2012; Shalev et al., 2009). As recently shown by Cavallina et al. (2022), the morpho-stratigraphic variability of the Venice coastal plain can be a key factor in the distribution of groundwater salinity. Here, small lithological variabilities were found to constrain the groundwater dynamics, affecting the freshwater-saltwater exchange. The same results were found in the southern portion of the Po Delta (Italy), where back barrier depositional facies were linked to a significant increase of groundwater salinity at shallow depths (Colombani et al., 2017; Di Giuseppe et al., 2014). In absence of dedicated multi-level samplers, to prove the concept express by Cavallina et al. (2022), a viable technique is the porewater extraction from sediment cores via batch experiments (Jiao et al., 2010). Batch experiments can be used to investigate the origin of groundwater salinity, especially analyzing non-reactive species such as chloride (Cl^-) and bromide (Br^-) that are not involved in redox reactions and thus could be considered environmental tracers (Cook and Herczeg, 2012).

The aim of this study is to highlight the strengths and weaknesses of porewater extraction as a method to assess the origin of salinity in coastal aquifers. This is a pivotal step since a correct understanding of the different sources of salinity may lead to a well-balanced water resources management in coastal aquifers, while often only actual seawater salinity is considered in management strategies (Hussain et al., 2019). The southern coastal area of the Venice Lagoon (Italy) was selected to test the proposed approach. For this purpose, sediment samples were collected at different depths and locations in the study area and the results from solute release in batch experiments were validated through sedimentary facies associations and hydrogeological information to unravel the salinity origin and the morpho-stratigraphic control on groundwater circulation.

2. Study area

The study area is located in the northern Adriatic coastal plain at the southern edge of the Venice Lagoon (Italy), in a low-lying agricultural region immediately south of the lower Brenta and Bacchiglione rivers (Fig. 1). The physiographic features of this region are the result of a combination of natural processes and human interventions, including land subsidence (Tosi et al., 2016), river diversions (Parrinello et al., 2021; Bondesan and Furlanetto, 2012), and hydraulic land reclamation carried out in the first three decades of the last century (Frascaroli et al., 2021). Due to the severe land subsidence associated with the oxidation of peat deposits (Gambolati et al., 2005), land elevations are now between −4 and −1 m above sea level (a.s.l.). Only the riverbanks of watercourses connected to the sea are a few meters a.s.l. The elevation differences in the area, originally due to the morphology of ancient marshes, lagoons, channel systems, coastal ridges, and coastal dunes before hydraulic land reclamation (Rizzetto et al., 2003), have been exacerbated in the last century by different land subsidence (Tosi et al., 2016). This critical Polder-like morphology represents a major hydrogeological hazard, especially for flooding and groundwater salinization (Da Lio et al., 2015; Tosi et al., 2022), with serious environmental and economic consequences (Torresan et al., 2012).

The water table is kept below sea level by a network of reclamation canals connected to pumping stations that drain the excess water into the lagoon, rivers, and sea. The water table fluctuates seasonally between 0.4 and 0.8 m below ground surface (i.e., between −2.4 and −2.8 m a.s.l.), depending on agricultural activities. The aquifer shows background values of EC ranging from 45 to 25 mS/cm, which decrease with increasing distance from the lagoon southward (Lovrinović et al., 2021). Precipitation significantly mitigates the high background levels of saline water in shallow unconfined aquifers, especially in the upper part of the aquifer associated with the paleochannel and coastal paleoridge systems. The influence of daily tidal variations on groundwater salinity is negligible, as is the influence on the water table since this is regulated by pumping stations. Contra wise, the influence of the Brenta, Bacchiglione, and Canal Morto rivers is evident during prolonged drought and high rainfall periods, with seawater ingression during droughts and freshwater flushing in wet periods.

The hydro-stratigraphic architecture in the study area is made up of sedimentary deposits of Late Pleistocene and Holocene age. The relationship between the subsurface architecture and the near-surface portion of the aquifer system is shown in Fig. 1. The Pleistocene sedimentary sequence is associated with the sea-level lowstand and consists of alluvial sands, silts, and clays deposited during the Last Glacial Maximum (LGM) (Donnici et al., 2012) when sea level was roughly 110–120 m lower than today (Storms et al., 2008). The uppermost Pleistocene aquifer consists of fluvial sands bounded above by a regionally extensive aquiclude of overconsolidated clayey deposits, a paleosol called *Caranto* (Donnici et al., 2011). The Holocene depositional units comprise a thin sedimentary sequence related to marine transgression, consisting of back barrier deposits, which is overlaid by the marine highstand sedimentary sequence. This sequence is related to the progradation of fluvio-deltaic systems, and consists of prodelta, delta front/littoral and delta plain/lagoon deposits (Zecchin et al., 2009; Tosi et al., 2009). The most important phreatic aquifer is associated to the littoral deposits, which extend on a regional scale. Other aquifers of local extent are associated to paleochannel systems and ancient littoral ridges.

3. Materials and methods

Nine sediment cores (MoST1, MoST2, MoST3, MoST4, MoST5, MoSTN, MoSTS, MoSTE, MoSTW) were provided by the EU projects MoST and SeCure. The locations of the cores were chosen to capture the variability of the subsurface on a local scale, including the paleochannels and interbasins shown in Fig. 1. The selection of samples for each core was done in the field, collecting a sample at each macroscopic

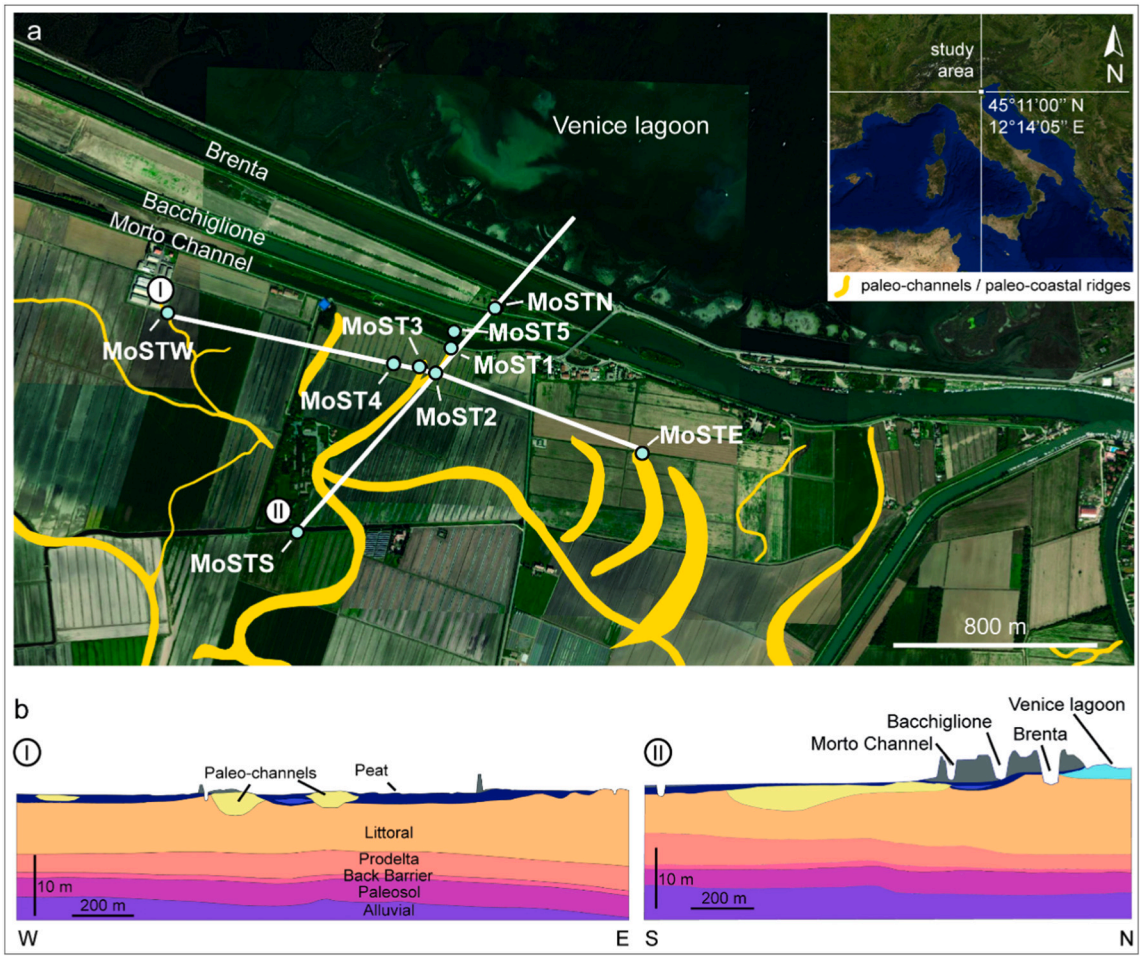

Fig. 1. (a) Satellite image of the study area showing the locations of MoST wells and sediment cores. The main sandy geomorphological structures are highlighted in yellow. (b) Geological cross-sections showing depositional units.

change in grain size, color, or presence of fragments (shells and/or vegetation).

Analysis of sedimentary cores in terms of lithology, grain size, sedimentary structures, color, and sorting as well as the presence of fossils, vegetal remains, and bioturbation, allowed the identification of facies associations (FA), each revealing different paleoenvironments (Cavallina et al., 2022). For the purposes of this paper, the facies associations described by Cavallina et al. (2022) have been grouped into the units U1, U2, U3 and U4 (Table 1). This simplification allowed a statistical representativeness of the data per unit, while maintaining the overall significance of the depositional environments where sediments were settled.

Sediment samples for the batch experiments were selected along cores to represent the stratigraphic distribution of the subsurface. They were stored in sediment boxes and subsampled in the field at each relevant macroscopic change in grain size, and then transported in the laboratory for analyses.

Batch leaching experiments were performed using the saturation soil extraction (SSE) method described by Schuwirth and Hofmann (2006) using deionized water (EC 10 ± 2 μS/cm, pH 6.5 ± 0.01, ORP 150 ± 10 mV) as liquid phase, while samples from sediment cores were used as solid phase. Batches were performed with a liquid/solid (L/S) ratio of 5:1 and the contact time was set at 80 days to allow the solid matrix to reach equilibrium with the liquid phase. Each batch was carried out in a Kartell container with a rectangular bottom (3.9 cm × 4.5 cm) and a height of 8.5 cm, which had a double stopper to seal off its content from the outside. To prevent algal growth, batches were kept in the dark, and in a temperature-controlled environment (25 °C ± 1 °C) and not stirred to mimic aquifer conditions.

TDS and pH (Supplementary dataset) were monitored each week using a HANNA multiparametric probe (HI98194) to check when equilibrium among solid and liquid phases was reached. The probe was calibrated before each measurement set for EC, pH and ORP using HANNA solution standards and the conversion factor among EC and TDS was 0.66 (APHA, 2017). While TDS or salinity are affected by reactions like mineral dissolution or organic matter oxidation, Cl^- and Br^- ions can be used as tracers to determine: i) the source of salinity in groundwater (Lorenzen et al., 2012; Park et al., 2005), ii) the genesis of deep saline waters, and iii) the degree of deep brines development (Stober and Bucher, 1999). Cl^- and Br^- are typically non-reactive ions because neither redox reactions nor low solubility minerals affect their contents. Consequently, the Cl^-/Br^- ratio must remain constant when Cl^- and Br^- originate from the same source (Alcalá and Custodio, 2008). This may help to distinguish between anthropogenic and natural causes of salinization (Hudak, 2003). After 80 days, water samples were collected from the batches and filtered to be analyzed for F^-, Cl^-, Br^-, NO_3^-, NO_2^-, SO_4^{2-}, and PO_4^{3-} with an ICS-1000 Dionex-ThermoFisher ion chromatography system equipped with an isocratic dual pump, an IonPac AS14A 4 × 250 mm column, an AG14A 4x50mm pre-column, and an ASRS-Ultra 4-mm self-suppressor for anions. NH_4^+ was quantified via Pharmacia 300 UV/VIS spectrophotometer with a Nessler reagent (Hach-Lange, UK). Mineral N was calculated summing the concentrations of NO_3^-, NO_2^-, and NH_4^+. Quality control (QC) samples were run every ten samples. The standard deviation for all QC samples run was

Table 1
Correspondences between the facies associations of Cavallina et al. (2022) and the unit associations used in the present work, with the number of samples collected.

Facies association from Cavallina et al., 2022	Description	Units in the present work and number of samples
Fa7	Peat and peaty clay layers of wetland areas. Back-barrier deposits	U1 (25)
Fa6	Medium to fine sand, laminated, containing shell fragments and plant remains, with a lenticular geometry base. Lagoonal (tidal) channel deposits	
Fa5	Well sorted, fine to medium sand, with abundant shells. Littoral deposits	U2 (37)
Fa4	Alternation of clayey and sandy silt with thin layers of fine laminated sand, with sparse mollusk shells. Prodelta deposits	U3 (32)
Fa3	Silt to silty sand deposits with coarse-grained sediments and shell lag above the erosive base. Transgressive back-barrier deposits	
Fa2	Clay to silty clay layers showing evident signs of pedogenesis. Alluvial pedogenized deposits referable to the *Caranto* paleosol	U4 (9)
Fa1	Medium beds of micaceous silty sand alternate with silt, with vegetal remains and roots. Alluvial deposits	

better than 4 %, whereas the accuracy which was 5 % for anions and 3 % for NH_4^+, reported as the average of the relative differences between the measured and known standards.

Porewater concentrations C_{pw} were calculated using the following formula:

$$C_{pw} = d^{*}C\left(\frac{\rho_b}{n}\right) \quad (1)$$

where d is the dilution factor due to the batch L/S; C is the concentration of the analyzed species in the liquid phase, ρ_b is the dry bulk density of the sample, and n is the total porosity of the sample. To assess the HI98194 probe stability, ever ten measurements in batches the probe was immersed in a calibration solution for QC. The accuracy of the batch measurements was ±1 % of reading for TDS, ±0.02 for pH and ±1.0 mV for ORP. The accuracy of d, ρ_b and n parameters was approximately ±1 % each, thus the overall uncertainties never exceeded ±5 % of the reported values for TDS, pH and ORP and never exceeded ±8 % for the C_{pw}. The end-members of non-reactive freshwater-saltwater mixing were the chemical composition of the Po River, Adige River, Venice Lagoon, and Adriatic seawater sourced from Colombani et al. (2017) and Gattacceca et al. (2009), which were used to infer different salinization mechanisms. The Cl^-/Br^- evaporation line was derived via linear interpolation over rain samples and U3 samples.

4. Results and discussion

4.1. Monitoring of TDS and pH

Equilibrium between the solid and liquid phases was achieved after 40 days, as testified by the negligible variations in TDS C_{pw} and pH values (Fig. 2). The TDS C_{pw} and pH values during the monitoring period are shown in Fig. 2a for the samples with the highest SO_4^{2-} and in Fig. 2b for the samples with peat content. Despite here only few samples are shown, all the others behaved in a very similar way, with a sharp TDS increase at the beginning followed by a plateau. All the data are reported in the Supplementary dataset.

In Fig. 2a, the samples show a similar decreasing pH trend and a corresponding increase of TDS due to the SO_4^{2-} released by mineral phases, like pyrite or gypsum. Pyrite is the main candidate for SO_4^{2-} release since it is largely present in the *Caranto* paleosol (Donnici et al., 2011) and ubiquitous in subsurface organic sediments of the Po plain (Amorosi et al., 2002; Di Giuseppe et al., 2014), while gypsum is seldom found in such depositional environments (Amorosi et al., 2002). In fact, pyrite oxidation was enhanced by the following reaction under basic conditions (Bonnissel-Gissinger et al., 1998), since pH values of the batches were generally between 7.5 and 8.5 during the monitoring period:

$$2FeS_{2(s)} + 3.5O_2 + H_2O \rightarrow Fe^{2+} + 2SO_4^{2-} + 2H^+ \quad (2)$$

From day 40 to 60, pH showed a slight increase due to the buffering effect of the C*aranto* paleosol (Donnici et al., 2011).

The peat samples have extremely low pH values (Fig. 2b), which can be attributed to the release of volatile and organic acids (Shotyk, 1988). Accordingly, the release occurred during the first days of monitoring after which TDS reached equilibrium values. The high release of SO_4^{2-} in these samples was due to the batch oxidative environment. In fact, besides triggering pyrite oxidation, the biodegradation of phenolic compounds present in the peaty horizons may have been accelerated by the presence of oxygen (Freeman et al., 2004). Through this process, SO_4^{2-} esters present in the peat matrix and bound to humic molecules can be converted into SO_4^{2-} (Chapman and Davidson, 2001).

4.2. Salinity origins

TDS values much higher than the actual mean Adriatic seawater salinity (i.e., 35,190 mg/L as reported by Grilli et al., 2020) have been measured for many samples even at shallow depths of about −4.0 m a.s.l. While Cl^- C_{pw} are generally lower than those of the actual mean Adriatic seawater (19,800 mg/L as reported by Colombani et al., 2017), and consistent with the mean Cl^- concentration of Mediterranean Sea (Khaska et al., 2013).

According to the relationship between TDS and Cl^- (Fig. 3a), the samples are not aligned along the sea-lagoon-freshwater mixing line, but they are all shifted above it, except for few cases. This means that TDS is not always related to chlorinity. The relationship between TDS and SO_4^{2-} (Fig. 3b) is a further confirmation of this finding, as the samples are almost entirely distributed below the freshwater-seawater mixing line. Here, the far higher than expected SO_4^{2-} C_{pw} are due to the pyrite and organic matter oxidation that occurred in the oxidative environment of the batch experiments. Thus, the major limitation of simply using TDS values derived from the porewater to distinguish among actual and paleoseawater or evapoconcentrated waters is the possible oxidation of organic materials that could bias the results in batch experiments.

The most superficial samples, related to delta plain/lagoon deposits, have higher Br^- and lower Cl^- values than the actual Adriatic Sea-Freshwater mixing line (U1 in Fig. 4a); therefore, the origin of Br^- is not marine but agriculturally derived (Samantara et al., 2015). In addition, most of the deep samples fall within the evaporation line rather than falling along the actual Adriatic Sea-Freshwater mixing line. This suggests that actual seawater intrusion is not the major driver of groundwater salinization, while other processes play a non-negligible role.

To identify the different endmembers and to disentangle the various mixing processes, the classical plots of Cl^-/Br^- vs Cl^-, and Br^- vs Br^-x10^3/Cl^- have been used. The Cl^-/Br^- molar ratio of the Adriatic seawater samples (red crosses in Fig. 4b) is relatively scattered compared to the oceanic mean seawater of 655, due to the Po River's seasonal freshwater discharge that smooths the salinity of the Adriatic Sea close to the Po River delta (Artegiani et al., 1997). Only a few samples in this study had Cl^-/Br^- ratio values attributable to the

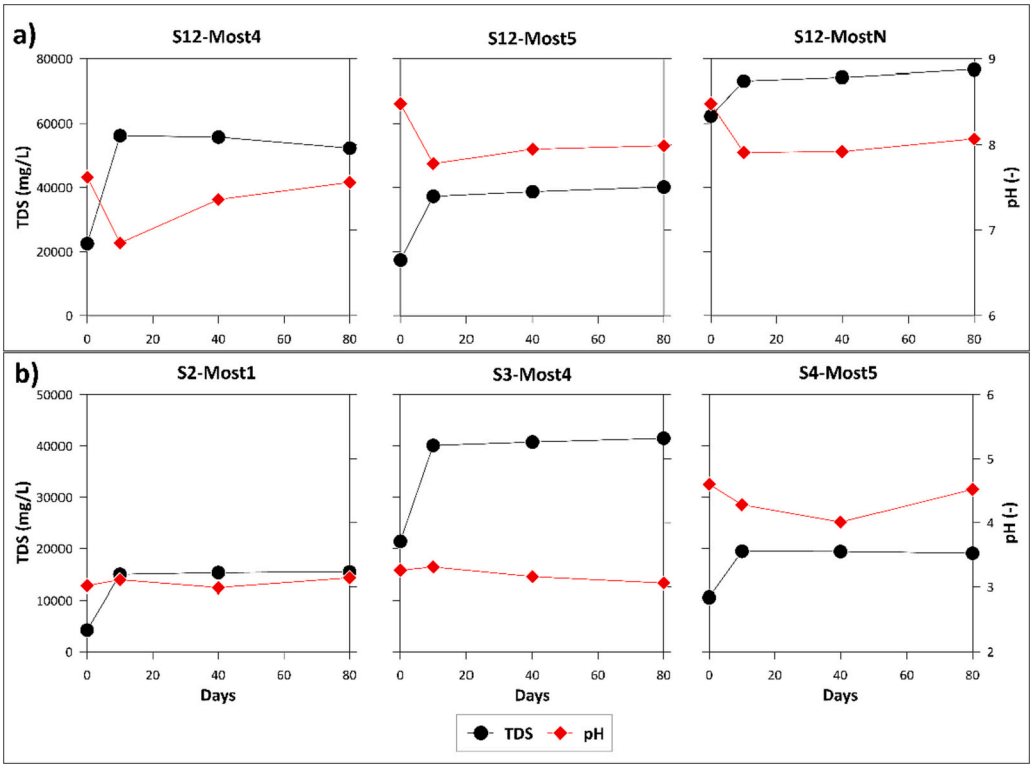

Fig. 2. TDS (mg/L) and pH trends of selected samples during the monitoring period: a) Samples with the highest SO_4^{2-} collected from −14 to −21 m a.s.l. and b) Peat samples collected from −2.5 to −5.0 m a.s.l.

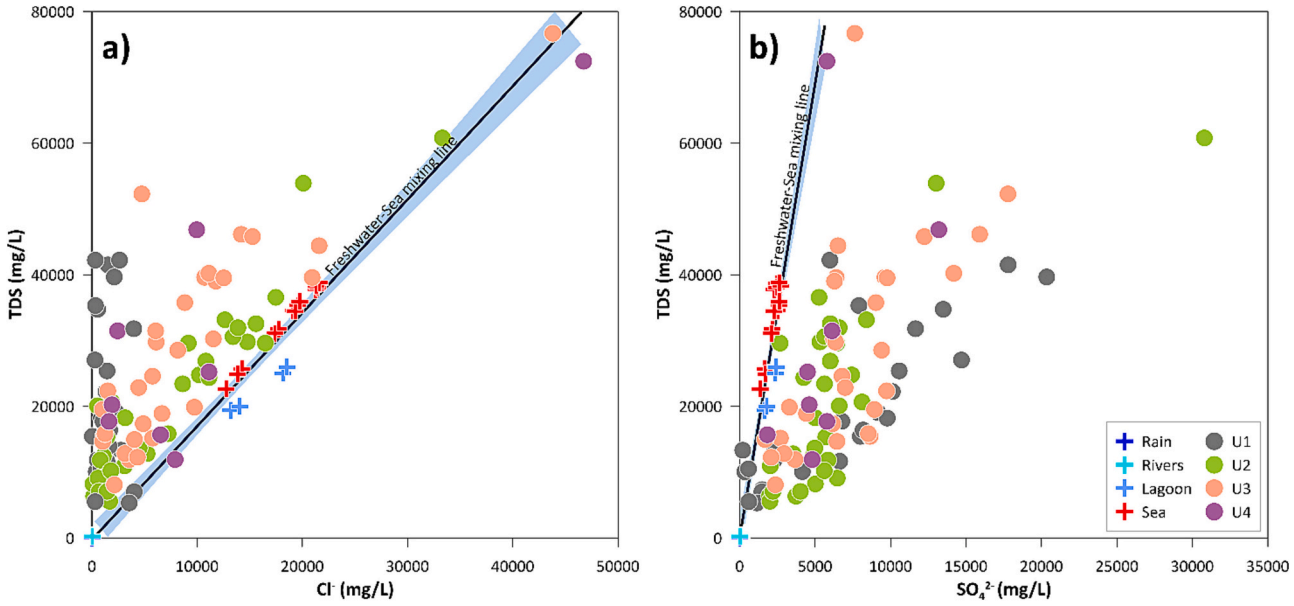

Fig. 3. Batches' water samples: a) TDS (mg/L) vs Cl^- (mg/l); b) TDS (mg/L) vs SO_4^{2-} (mg/l). The black dotted lines indicate the Sea-Lagoon-Freshwater mixing lines, and the blue areas indicate a 95 % confidence interval.

seawater or lagoon water intrusion and their mixing with freshwater endmembers (highlighted by the red arrow in Fig. 4). The deeper samples associated with LGM deposits (U4) and prodelta Holocene deposits (U3) are aligned at Cl^-/Br^- 900 ± 80 (Fig. 4b), as previously noted by Colombani et al. (2017), which has been related to the intrusion of paleo-seawater and mixing with evaporitic layers. Those with an extremely low Cl^-/Br^- ratio are instead linked to recharge of agricultural leaching, as attested by their shallow depth and the association to the youngest unit of the delta plain/lagoon deposits, while a few shallow samples encompassed high evaporation and are mixed with manure (U1 in Fig. 4b). These results are consistent with the management of this land that has been intensively cultivated since the late 1970s (Cavallina et al., 2022). Samples with extremely high Cl^-/Br^- ratio found in U4 were linked to halite dissolution, very poor in Br^- (Herrmann, 1972), formerly precipitated in lagoonal and marsh environments characterized by shallow ponds in a drier than actual climate, plausibly during the

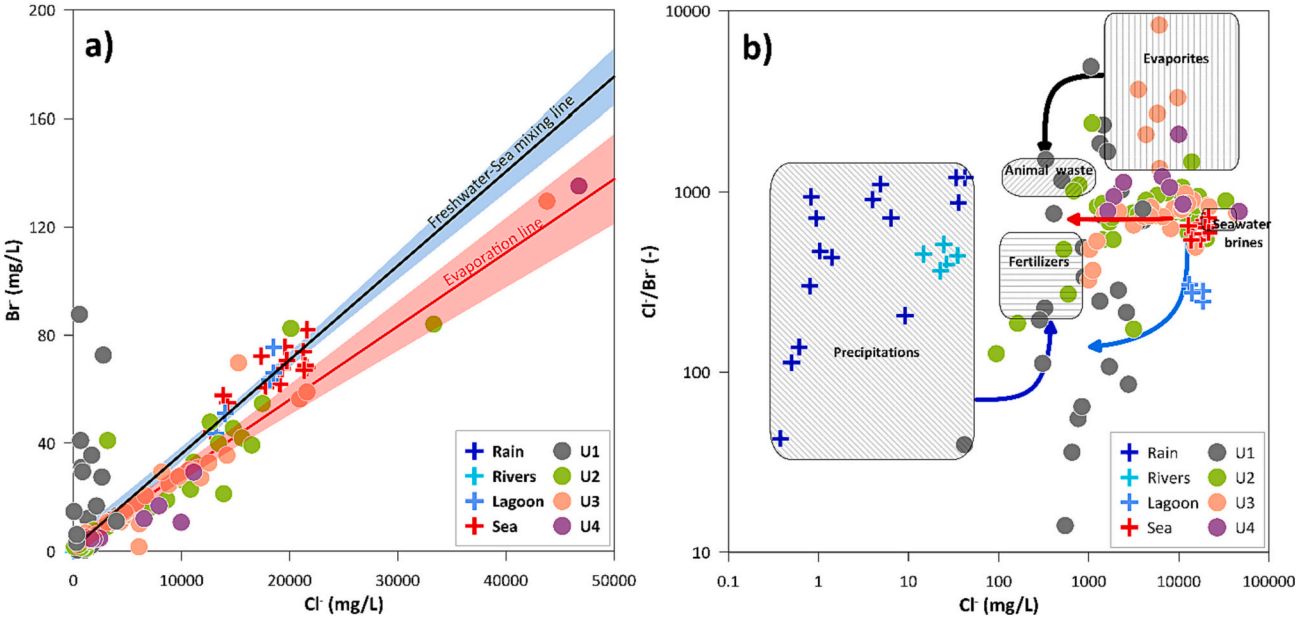

Fig. 4. Batches' water samples: a) Br^- (mg/L) vs Cl^- (mg/l). The black line indicates the Sea-Lagoon-Rivers-Rain mixing line and the blue area indicates a 95 % confidence interval. The red line indicates the evaporation line, and the pink area indicates a 95 % confidence interval. b) Cl/Br molar ratio (–) vs Cl^- (mg/l). The arrows indicate the different mixing lines among end-members. Rectangular boxes are reported merging Alcalá and Custodio (2008), Panno et al. (2006), and Sun et al. (2019).

post LGM marine transgression. Mixing processes have then diluted the original hypersaline waters with recharge waters. In fact, most samples are located between the evaporites leaching box and the Adriatic seawater samples (Fig. 4b).

Further validation that most of the salinity do not originate from actual seawater intrusion and not even from recently evaporated waters from the Venice lagoon but is rather due to paleosalinity (for the deepest samples) and mixing of different sources (for the shallow samples) is provided in Fig. 5a. In the Br^- vs Br^-x10^3/Cl^- plot, the samples are not aligned along the halite-seawater line experiment carried out by Sun et al. (2019), which depicts the actual seawater evaporation trend. Instead, they exhibited evapoconcentration trends like those found for seawater evaporation, but starting from continental water (Zhang et al., 2018). Since continental waters have much lower Br^- content respect to seawater and higher Br^-x10^3/Cl^-, they are aligned in a shifted line respect to the actual seawater evaporation line. From Fig. 5b, it is evident that the Br^-x10^3/Cl^- molar ratio increased in the shallower facies U1 compared to the deeper facies due to the anthropogenic input

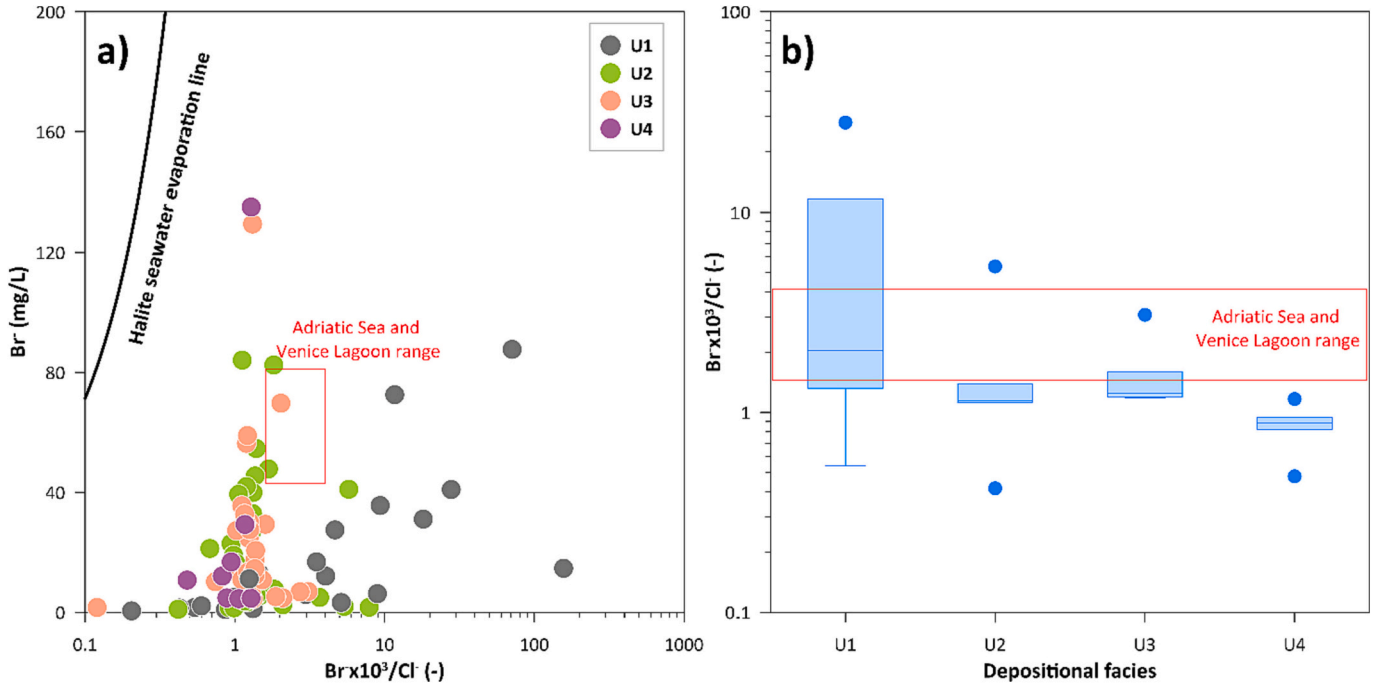

Fig. 5. a) Plot of Br (mg/l) vs Br^-x10^3/Cl^- molar ratio (–) for the different depositional facies. The black line indicates the fitted line of a halite-seawater experiment reported by Sun et al. (2019) and the red rectangles indicate the ranges in actual sea and lagoon. b) Box-Whisker plot of Br^-x10^3/Cl^- molar ratio (–) for each depositional facies, with blue dots highlighting outliers.

from agricultural activities, with a broad range of scattered values. In contrast, in the deeper depositional facies U4 the values are much less scattered, while facies U2 and U3 are also affected by mixing with actual seawater.

4.3. Hydro-stratigraphic model paired with salt origin

The Cl^- C_{pw} and Cl^-/Br^- values have been analyzed in relation to subsurface depth and facies units (Fig. 6) to depict a simple conceptual model of freshwater-saltwater exchange coupled with groundwater salinity origins. This conceptual model is also discussed to highlight the strengths and limitations of sediment core batch analysis.

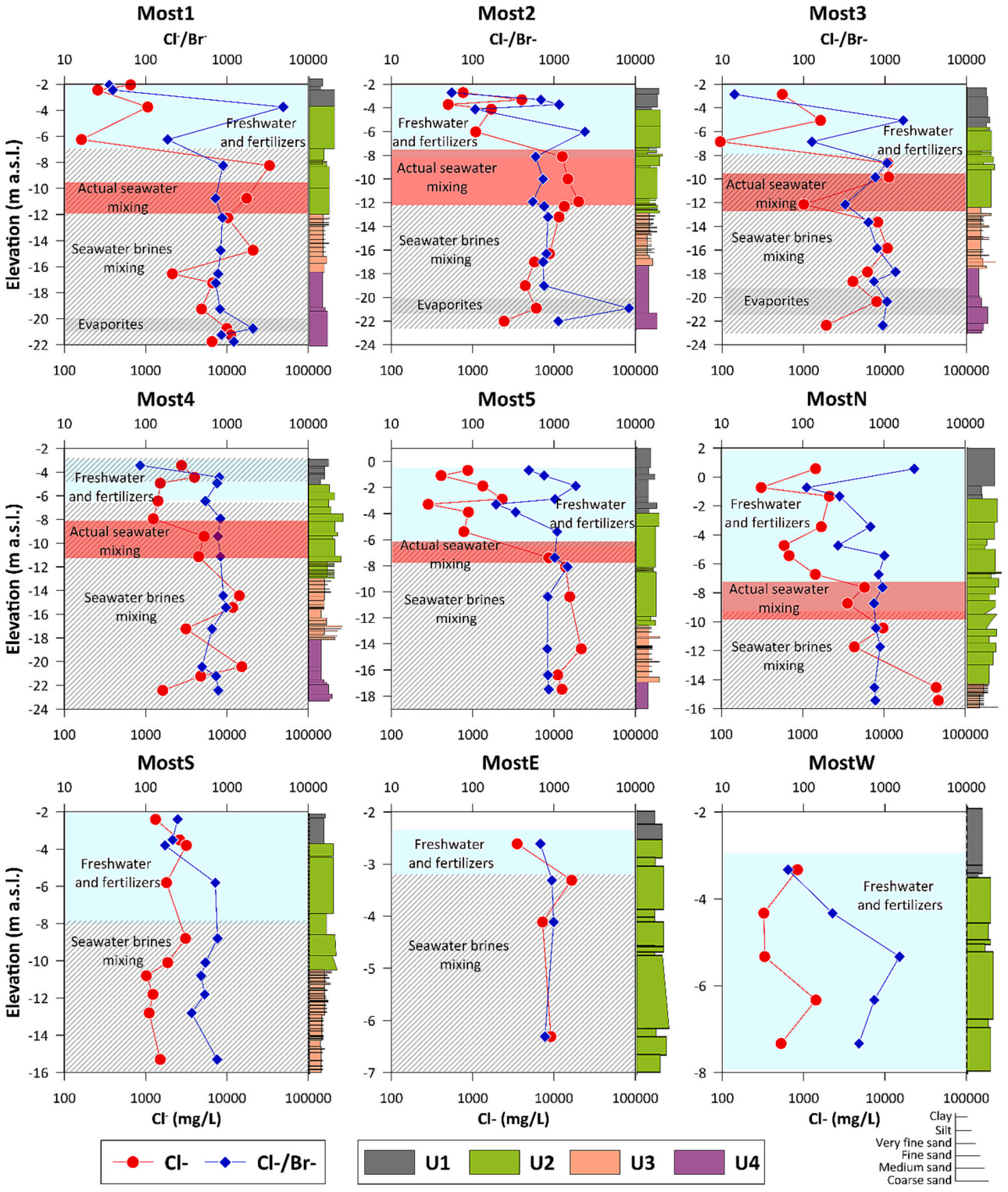

Fig. 6. Cl^- C_{pw} and Cl^-/Br^- values measured in the sedimentary cores and their salinity origins. The depositional units (U) and sediments' grain size are shown. Note that the scale of vertical and horizontal axes varies.

The shallowest facies associated with reworked deposits and the superficial facies of the morpho-stratigraphic sequence characterized by peat and clays (lagoon/delta plain deposits of U1) show the lowest values of Cl^- C_{pw} (Fig. 6), due to the infiltrating freshwater from canals and rainwater. The sandy deposits with medium-high permeability (littoral and delta front deposits of U2) are instead characterized by high variability, with increasing Cl^- C_{pw} downward. Moving downward, the alternation of clayey and sandy silt with thin layers of fine laminated sand with low permeability (mostly prodelta deposits of U3) exhibited some peaks in Cl^- C_{pw}, considering the trends of the overlying layer. The silty and sandy deposits topped by overconsolidated clay deposits with extremely low permeability (the alluvial LGM deposits of U4), again showed a decrease in Cl^- C_{pw} compared to U3.

The Cl^-/Br^- values show a more homogeneous trend along the core profiles with respect to Cl^-, with values around 900 as previously described, except for the samples from the evaporitic layers, which show remarkably high values. The recently recharged waters of agricultural origin are located in the upper part of the aquifer and do not exceed −8 m a.s.l. Below the shallow (recent) groundwater lies a thin wedge of actual seawater intruded in the most permeable layers at elevation among −8 and −12 m a.s.l. Below this thin layer a mixing between actual and paleo-seawater is present, while at the base of this lens can be found the endmember of evaporitic origin comprised among −20 and −22 m a.s.l., recognized only in 3 of the 9 cores analyzed. The latter has contributed to salinizing the whole aquitard (U3) via diffusion processes, given that the permeability of these sediments is low due to its silty matrix. When in doubt if mixing waters were from agricultural sources or from peaty layers the mineral N was checked, and if above 500 mg/L it was ascribed to peat release (see Supplementary database for the mineral N data), while PO_4^{3-} was of little use to delineate possible agricultural sources since it was always below detection limits in all the samples due to its low solubility in oxidizing environments (Di Giuseppe et al., 2014). Also the F^- C_{pw} supported the evapoconcentration of seawater with abrupt increases especially in U3 within low permeability layers characterized by higher than actual seawater Cl^-/Br^- values (see Supplementary database for the F^- C_{pw}), but given the high reactivity of F^- the relationship was complex with peaks also in peaty horizons were F^- may accumulate via adsorption or precipitation processes. Moreover, the confined aquifer has a hydraulic head higher than the Adriatic Sea and is therefore artesian in this area (Teatini et al., 2009). Thus, it can support slow diffuse upward gradients that may have led to mixing between the evaporitic porewaters and the less saline recharge waters from rivers and rainfall. This behavior is quite common in layered sedimentary coastal aquifers and aquitards characterized by polder-like environments (Caschetto et al., 2016; de Louw et al., 2010; Kuang et al., 2015). The same aspect was also stressed in study on the southern Venice coastal aquifers (Gattacceca et al., 2009), where the authors noted the importance of upward groundwater fluxes favored by the network of reclamation channels, which in turn depressed the phreatic water table.

Fig. 7 shows the overall conceptual model representing the exchange between the watercourses and the groundwater, together with the salinization mechanisms in the context of the hydrostratigraphic environment units, i.e., the saltwater contamination from the deeper evaporitic layer, the circulation of fresh-brackish-salt water from the rivers and toward the reclamation channels, and the present-day saltwater intrusion from the Venice lagoon. From a hydrogeological point of view, the groundwater head gradient is gently sloping from the Venice lagoon and rivers toward the reclamation canals network (Fig. 7), continuously drained by the pumping stations that pump back the water into the rivers. This short-circuit allow brackish and saline waters of the Venice lagoon to seep into the highly permeable sandy layers of U2 unit. While the confined aquifer provides the vertical head gradient that allows the slow upward migration of brines through the aquitard lenses of U3 and U4 (Fig. 7).

Previous studies based on geophysical surveys (de Franco et al., 2009; Teatini et al., 2011; Tosi et al., 2018; Viezzoli et al., 2010), water monitoring (Carbognin and Tosi, 2003; Lovrinović et al., 2021), and

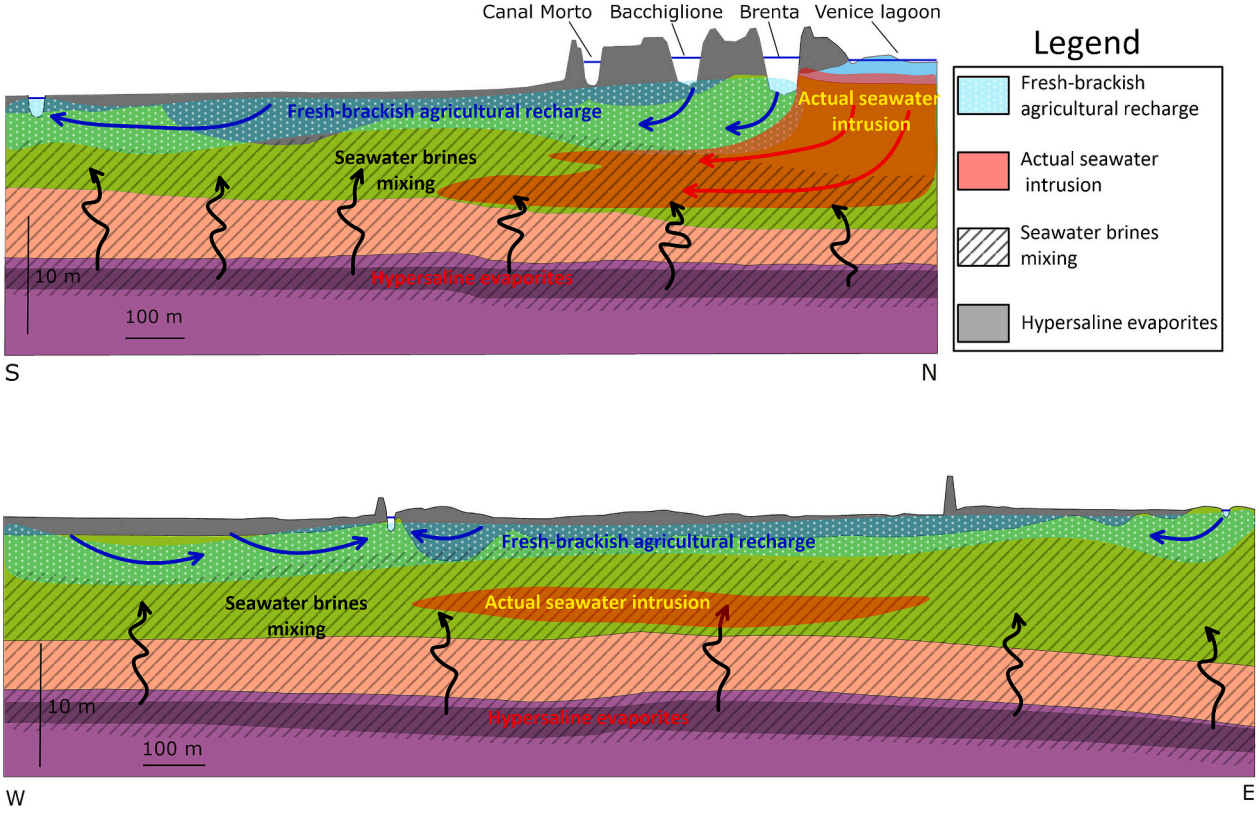

Fig. 7. Schematic sketch of the salinization mechanisms and origin in the studied area, based on the porewater profiles.

numerical modeling (Teatini et al., 2009) in this area were pivotal in delineating saltwater-freshwater relationships in both unconfined and confined aquifers and the lateral extent and temporal variability of saline groundwater, but they were unable to recognize different sources of salinity. While a recent study (Zancanaro et al., 2020) performed in this site using vadose zone data, highlighted the different origins of porewaters with two main sources: i) the actual seawater intrusion from the Venice lagoon, and ii) the salinity derived from peaty sediments. The Cl^-/Br^- values found by Zancanaro et al. (2020) are in good agreement with the ones here found at deeper depths and in distinct locations, independently proving the results of this study.

The large-scale characterization via stable isotopes and Cl^-/Br^- values of Gattacceca et al. (2009) recognized the relative importance of evaporated groundwater endmembers. However, they were roughly able to quantify the evaporated groundwater contribution due to the long screen boreholes employed, that often obliterate the true aquifer mixing processes. For this type of analysis, given the complex hydrostratigraphic setting and multiple sources of salinization, the employment of high vertical resolution multi-level samples is fundamental for a better understanding of the salinization processes taking place in the area. In absence of dedicated multi-level samplers monitoring wells, the proposed strategy of analyzing C_{pw} via batch experiments and compare them with the unit associations may allow to distinguish among paleo and actual seawater origins, while standard integrated depth sampling often led to biased or even misleading conceptual models of coastal aquifer salinization (Colombani et al., 2016). This could provide crucial information for the development of numerical transport models that could support local authorities in the proper management of the water resources (Huang and Chiu, 2018; Werner and Gallagher, 2006) also in view of the predicted decreased recharge in Mediterranean coastal areas (Busico et al., 2021). Limitations of this method arise from the availability of continuous core logs and their sedimentological/stratigraphical interpretation and from the batches' oxidative environment that may alter the C_{pw} TDS. Although, this could be overcome by using environmental tracers like Cl^- and Br^- not affected by redox reactions, or alternatively preserving the redox state of sediments via N_2 flushing and anaerobic incubations (Jiao et al., 2010), but the latter technique is extremely expensive and need highly specialized equipment.

5. Conclusions

This study shows that more than one hydrologic process contributes to groundwater salinization of the Venice lagoon coastal aquifer. Here, Br^- and Cl^- porewater concentrations coupled with the analysis of depositional unit associations helped to determine the different sources of salinity. The Br/Cl molar ratio and its reciprocal detected in the shallower samples showed that the causes of groundwater salinization in the shallow aquifer are most likely due to agricultural activities and not to the actual seawater intrusion, while the actual seawater wedge forms a thin layer of 2–3 m between the agricultural water (at the top) and the evaporated paleowater (at the bottom). The main limitation of this approach concerns the biased TDS values derived from the porewater, which were affected by the oxidation of peat and pyrite in the batches. Therefore, only non-reactive environmental tracers shall be used to delineate salinity profiles of porewaters.

In summary, the proposed approach has been designed to determine the origin of groundwater salinity in coastal areas to discriminate among actual seawater intrusion and other causes, such as trapped paleoseawater or evapoconcentrated salts (halides) in transitional environments. The results of this study provide useful information to properly understand and manage groundwater salinization in coastal aquifers where actual seawater intrusion is often erroneously considered to be the main driver, leading to misguided land management policies that do not correctly address and effectively minimize the issue of salinization.

Supplementary data to this article can be found online at https://doi.org/10.1016/j.scitotenv.2023.167058.

CRediT authorship contribution statement

Luigi Alessandrino: Investigation, Software, Formal analysis, Data curation, Visualization, Writing – original draft. **Mattia Gaiolini:** Formal analysis, Data curation, Visualization. **Francisco Aldo Cellone:** Formal analysis, Investigation. **Nicolò Colombani:** Conceptualization, Methodology, Software, Writing – review & editing, Visualization. **Micòl Mastrocicco:** Conceptualization, Validation, Writing – review & editing. **Marta Cosma:** Formal analysis, Software, Visualization. **Cristina Da Lio:** Formal analysis, Software, Visualization. **Sandra Donnici:** Formal analysis, Writing – review & editing. **Luigi Tosi:** Writing – review & editing, Funding acquisition, Project administration.

Declaration of competing interest

The authors declare that they have no known competing financial interests or personal relationships that could have appeared to influence the work reported in this paper.

Data availability

Data will be made available on request.

Acknowledgments

This research was supported by the EU co-financing the Interreg Italy–Croatia CBC Programme 2014–2020 (Cluster 2, Specific Objective 2.1) through the European Regional Development Fund as a part of the project “Saltwater intrusion and climate change: monitoring, countermeasures and informed governance” (SeCure AID: 10419304). The authors also acknowledge the project “Monitoring seawater intrusion in coastal aquifers and testing pilot projects for its mitigation” (MoST AID: 10047743). The authors would like to thank Mirco Marcellini for the IC analyses.

References

Alcalá, F.J., Custodio, E., 2008. Using the Cl/Br ratio as a tracer to identify the origin of salinity in aquifers in Spain and Portugal. J. Hydrol. 359, 189–207. https://doi.org/10.1016/j.jhydrol.2008.06.028.

American Public Health Association (APHA), 2017. Standard Methods for the Examination of Water and Wastewater, 23rd edition. American Public Health Association, American Water Works Association, and Water Environment Federation, Washington DC. (1268 pp. ISBN: 978-0-87553-287-5).

Amorosi, A., Centineo, M.C., Dinelli, E., Lucchini, F., Tateo, F., 2002. Geochemical and mineralogical variations as indicators of provenance changes in Late Quaternary deposits of SE Po Plain. Sediment. Geol. 151 (3–4), 273–292. https://doi.org/10.1016/S0037-0738(01)00261-5.

Artegiani, A., Bregant, D., Paschini, E., Pinardi, N., Raicich, F., Russo, A., 1997. The Adriatic sea general circulation. Part I: air-sea interactions and water mass structure. J. Phys. Oceanogr. 27, 1492–1514. https://doi.org/10.1175/1520-0485(1997)027<1492:TASGCP>2.0.CO;2.

Ashraf, B., AghaKouchak, A., Alizadeh, A., 2017. Quantifying anthropogenic stress on groundwater resources. Sci. Rep. 7, 12910. https://doi.org/10.1038/s41598-017-12877-4.

Barbecot, F., Marlin, C., Gibert, E., Dever, L., 2000. Hydrochemical and isotopic characterisation of the Bathonian and Bajocian coastal aquifer of the Caen area (northern France). Appl. Geochem. 15, 791–805. https://doi.org/10.1016/S0883-2927(99)00088-8.

Bondesan, A., Furlanetto, P., 2012. Artificial fluvial diversions in the mainland of the lagoon of Venice during the 16th and 17th centuries inferred by historical cartography analysis. Géomorphologie 2, 175–200. https://doi.org/10.4000/geomorphologie.9815.

Bonnissel-Gissinger, P., Alnot, M., Ehrhardt, J.-J., Behra, P., 1998. Surface oxidation of pyrite as a function of pH. Environ. Sci. Technol. 32, 2839–2845. https://doi.org/10.1021/es980213c.

Busico, G., Ntona, M.M., Carvalho, S.C., Patrikaki, O., Voudouris, K., Kazakis, N., 2021. Simulating future groundwater recharge in coastal and inland catchments. Water Resour. Manag. 35 (11), 3617–3632. https://doi.org/10.1007/s11269-021-02907-2.

Carbognin, L., Tosi, L., 2003. Il Progetto ISES per l’Analisi dei processi di intrusione salina e subsidenza nei territori meridionali delle Provincie di Padova e Venezia. Istituto per lo Studio della Dinamica delle Grandi Masse, Venice, Italy.

Cartwright, I., Weaver, T.R., Fulton, S., Nichol, C., Reid, M., Cheng, X., 2004. Hydrogeochemical and isotopic constraints on the origins of dryland salinity, Murray

Basin, Victoria, Australia. Appl. Geochem. 19, 1233–1254. https://doi.org/10.1016/j.apgeochem.2003.12.006.
Caschetto, M., Colombani, N., Mastrocicco, M., Petitta, M., Aravena, R., 2016. Estimating groundwater residence time and recharge patterns in a saline coastal aquifer. Hydrol. Process. 30 (22), 4202–4213. https://doi.org/10.1002/hyp.10942.
Cavallina, C., Bergamasco, A., Cosma, M., Da Lio, C., Donnici, S., Tang, C., Tosi, L., Zaggia, L., 2022. Morpho-sedimentary constraints in the groundwater dynamics of low-lying coastal area: the southern margin of the Venice lagoon, Italy. Water 14 (17), 2717. https://doi.org/10.3390/w14172717.
Chapman, S.J., Davidson, M.S., 2001. ^{35}S-sulphate reduction and transformation in peat. Soil Biol. Biochem. 33, 593–602. https://doi.org/10.1016/S0038-0717(00)00201-7.
Colombani, N., Volta, G., Osti, A., Mastrocicco, M., 2016. Misleading reconstruction of seawater intrusion via integral depth sampling. J. Hydrol. 536, 320–326. https://doi.org/10.1016/j.jhydrol.2016.03.011.
Colombani, N., Cuoco, E., Mastrocicco, M., 2017. Origin and pattern of salinization in the Holocene aquifer of the southern Po Delta (NE Italy). J. Geochem. Explor. 175, 130–137. https://doi.org/10.1016/j.gexplo.2017.01.011.
Cook, P.G., Herczeg, A.L., 2012. Environmental Tracers in Subsurface Hydrology. Springer, New York, NY. https://doi.org/10.1007/978-1-4615-4557-6.
Da Lio, C., Tosi, L., 2019. Vulnerability to relative sea-level rise in the Po river delta (Italy). Estuar. Coast. Shelf Sci. 228, 106379. https://doi.org/10.1016/j.ecss.2019.106379.
Da Lio, C., Carol, E., Kruse, E., Teatini, P., Tosi, L., 2015. Saltwater contamination in the managed low-lying farmland of the Venice coast, Italy: an assessment of vulnerability. Sci. Total Environ. 533, 356–369. https://doi.org/10.1016/j.scitotenv.2015.07.013.
de Franco, R., Biella, G., Tosi, L., Teatini, P., Lozej, A., Chiozzotto, B., Giada, M., Rizzetto, F., Claude, C., Mayer, A., Bassan, V., Gasparetto-Stori, G., 2009. Monitoring the saltwater intrusion by time lapse electrical resistivity tomography: the Chioggia test site (Venice Lagoon, Italy). J. Appl. Geophys. 69 (3–4), 117–130. https://doi.org/10.1016/j.jappgeo.2009.08.004.
de Louw, P.G.B., Essink, G.H.P.O., Stuyfzand, P.J., van der Zee, S.E.A.T.M., 2010. Upward groundwater flow in boils as the dominant mechanism of salinization in deep polders, The Netherlands. J. Hydrol. 394, 494–506. https://doi.org/10.1016/j.jhydrol.2010.10.009.
Di Giuseppe, D., Faccini, B., Mastrocicco, M., Colombani, N., Coltorti, M., 2014. Reclamation influence and background geochemistry of neutral saline soils in the Po River Delta Plain (Northern Italy). Environ. Earth Sci. 72 (7), 2457–2473. https://doi.org/10.1007/s12665-014-3154-4.
Donnici, S., Serandrei-Barbero, R., Bini, C., Bonardi, M., Lezziero, A., 2011. The caranto paleosol and its role in the early urbanization of Venice. Geoarchaeology 26, 514–543. https://doi.org/10.1002/gea.20361.
Donnici, S., Serandrei-Barbero, R., Canali, G., 2012. Evidence of climatic changes in the Venetian Coastal Plain (Northern Italy) during the last 40,000 years. Sediment. Geol. 281, 139–150. https://doi.org/10.1016/j.sedgeo.2012.09.003.
Frascaroli, F., Parrinello, G., Root-Bernstein, M., 2021. Linking contemporary river restoration to economics, technology, politics, and society: perspectives from a historical case study of the Po River Basin, Italy. Ambio 50 (2), 492–504. https://doi.org/10.1007/s13280-020-01363-3.
Freeman, C., Ostle, N.J., Fenner, N., Kang, H., 2004. A regulatory role for phenol oxidase during decomposition in peatlands. Soil Biol. Biochem. 36, 1663–1667. https://doi.org/10.1016/j.soilbio.2004.07.012.
Gambolati, G., Putti, M., Teatini, P., Camporese, M., Ferraris, S., Gasparetto Stori, G., Nicoletti, V., Silvestri, S., Rizzetto, F., Tosi, L., 2005. Peat land oxidation enhances subsidence in the Venice watershed. Eos 86, 217–220. https://doi.org/10.1029/2005EO230001.
Gattacceca, J.C., Vallet-Coulomb, C., Mayer, A., Claude, C., Radakovitch, O., Conchetto, E., Hamelin, B., 2009. Isotopic and geochemical characterization of salinization in the shallow aquifers of a reclaimed subsiding zone: the southern Venice Lagoon coastland. J. Hydrol. 378 (1–2), 46–61. https://doi.org/10.1016/j.jhydrol.2009.09.005.
Giambastiani, B.M.S., Kidanemariam, A., Dagnew, A., Antonellini, M., 2021. Evolution of salinity and water table level of the phreatic coastal aquifer of the Emilia Romagna region (Italy). Water 13 (3), 372. https://doi.org/10.3390/w13030372.
Grilli, F., Accoroni, S., Acri, F., Bernardi, Aubry F., Bergami, C., Cabrini, M., Campanelli, A., Giani, M., Guicciardi, S., Marini, M., Neri, F., Penna, A., Penna, P., Pugnetti, A., Ravaioli, M., Riminucci, F., Ricci, F., Totti, C., Viaroli, P., Cozzi, S., 2020. Seasonal and interannual trends of oceanographic parameters over 40 years in the northern Adriatic Sea in relation to nutrient loadings using the EMODnet chemistry data portal. Water 12 (8), 2280. https://doi.org/10.3390/w12082280.
Herrmann, A.G., 1972. Bromine distribution coefficients for halite precipitated from modern sea water under natural conditions. Contrib. Mineral. Petrol. 37, 249–252. https://doi.org/10.1007/BF00373073.
Huang, P.S., Chiu, Y.C., 2018. A simulation-optimization model for seawater intrusion management at Pingtung coastal area, Taiwan. Water 10 (3), 251. https://doi.org/10.3390/w10030251.
Hudak, P.F., 2003. Chloride/bromide ratios in leachate derived from farm-animal waste. Environ. Pollut. 121 (1), 23–25. https://doi.org/10.1016/S0269-7491(02)00211-7.
Hussain, M.S., Abd-Elhamid, H.F., Javadi, A.A., Sherif, M.M., 2019. Management of seawater intrusion in coastal aquifers: a review. Water 11 (12), 2467. https://doi.org/10.3390/w11122467.
Jiao, J.J., Wang, Y., Cherry, J.A., Wang, X., Zhi, B., Du, H., Wen, D., 2010. Abnormally high ammonium of natural origin in a coastal aquifer-aquitard system in the Pearl River Delta, China. Environ. Sci. Technol. 44 (19), 7470–7475. https://doi.org/10.1021/es1021697.
Khaska, M., Salle, C.L.G.L., Lancelot, J., Team, A., Mohamad, A., Verdoux, P., Noret, A., Simler, R., 2013. Origin of groundwater salinity (current seawater vs. saline deep water) in a coastal karst aquifer based on Sr and Cl isotopes. Case study of the La Clape massif (southern France). Appl. Geochem. 37, 212–227. https://doi.org/10.1016/j.apgeochem.2013.07.006.
Kuang, X., Jiao, J.J., Liu, K., 2015. Numerical studies of vertical Cl^-, δ^2H and $\delta^{18}O$ profiles in the aquifer–aquitard system in the Pearl River Delta, China. Hydrol. Process. 29, 4199–4209. https://doi.org/10.1002/hyp.10483.
Li, C., Gao, X., Li, S., Bundschuh, J., 2020. A review of the distribution, sources, genesis, and environmental concerns of salinity in groundwater. Environ. Sci. Pollut. Res. 27 (33), 41157–41174. https://doi.org/10.1007/s11356-020-10354-6.
Lorenzen, G., Sprenger, C., Baudron, P., Gupta, D., Pekdeger, A., 2012. Origin and dynamics of groundwater salinity in the alluvial plains of western Delhi and adjacent territories of Haryana State, India. Hydrol. Process. 26, 2333–2345. https://doi.org/10.1002/hyp.8311.
Lovrinović, I., Bergamasco, A., Srzić, V., Cavallina, C., Holjević, D., Donnici, S., Erceg, J., Zaggia, L., Tosi, L., 2021. Groundwater monitoring systems to understand sea water intrusion dynamics in the Mediterranean: the Neretva valley and the southern Venice coastal aquifers case studies. Water 13 (4), 561. https://doi.org/10.3390/w13040561.
Manivannan, V., Elango, L., 2019. Seawater intrusion and submarine groundwater discharge along the Indian coast. Environ. Sci. Pollut. Res. 26, 31592–31608. https://doi.org/10.1007/s11356-019-06103-z.
Mastrocicco, M., Colombani, N., 2021. The issue of groundwater salinization in coastal areas of the Mediterranean region: a review. Water 13 (1), 90. https://doi.org/10.3390/w13010090.
Mastrocicco, M., Giambastiani, B.M.S., Severi, P., Colombani, N., 2012. The importance of data acquisition techniques in saltwater intrusion monitoring. Water Resour. Manag. 26, 2851–2866. https://doi.org/10.1007/s11269-012-0052-y.
Montety, V. de, Radakovitch, O., Vallet-Coulomb, C., Blavoux, B., Hermitte, D., Valles, V., 2008. Origin of groundwater salinity and hydrogeochemical processes in a confined coastal aquifer: case of the Rhône delta (Southern France). Appl. Geochem. 23, 2337–2349. https://doi.org/10.1016/j.apgeochem.2008.03.011.
Panno, S.V., Hackley, K.C., Hwang, H.H., Greenberg, S.E., Krapac, I.G., Landsberger, S., O'Kelly, D.J., 2006. Characterization and identification of Na-Cl sources in ground water. Groundwater 44, 176–187. https://doi.org/10.1111/j.1745-6584.2005.00127.x.
Park, S.-C., Yun, S.-T., Chae, G.-T., Yoo, I.-S., Shin, K.-S., Heo, C.-H., Lee, S.-K., 2005. Regional hydrochemical study on salinization of coastal aquifers, western coastal area of South Korea. J. Hydrol. 313, 182–194. https://doi.org/10.1016/j.jhydrol.2005.03.001.
Parrinello, G., Bizzi, S., Surian, N., 2021. The retreat of the delta: a geomorphological history of the Po River basin during the twentieth century. Water Hist. 13 (1), 117–136. https://doi.org/10.1007/s12685-021-00279-3.
Rizzetto, F., Tosi, L., Carbognin, L., Bonardi, M., Teatini, P., 2003. Geomorphic Setting and Related Hydrogeological Implications of the Coastal Plain South of the Venice Lagoon, Italy. IAHS-AISH Publication, pp. 463–470.
Samantara, M.K., Padhi, R.K., Satpathy, K.K., Sowmya, M., Kumaran, P., 2015. Groundwater nitrate contamination and use of Cl/Br ratio for source appointment. Environ. Monit. Assess. 187, 50. https://doi.org/10.1007/s10661-014-4211-x.
Schuwirth, N., Hofmann, T., 2006. Comparability of and alternatives to leaching tests for the assessment of the emission of inorganic soil contamination. J. Soils Sediments 6, 102–112. https://doi.org/10.1065/jss2005.10.149.
Shalev, E., Lazar, A., Wollman, S., Kington, S., Yechieli, Y., Gvirtzman, H., 2009. Biased monitoring of fresh water-salt water mixing zone in coastal aquifers. Groundwater 47, 49–56. https://doi.org/10.1111/j.1745-6584.2008.00502.x.
Shotyk, W., 1988. Review of the inorganic geochemistry of peats and peatland waters. Earth-Sci. Rev. 25 (2), 95–176. https://doi.org/10.1016/0012-8252(88)90067-0.
Stober, I., Bucher, K., 1999. Origin of salinity of deep groundwater in crystalline rocks. Terra Nova 11, 181–185. https://doi.org/10.1046/j.1365-3121.1999.00241.x.
Storms, J.E.A., Weltje, G.J., Terra, G.J., Cattaneo, A., Trincardi, F., 2008. Coastal dynamics under conditions of rapid sea-level rise: late Pleistocene to Early Holocene evolution of barrier–lagoon systems on the northern Adriatic shelf (Italy). Quat. Sci. Rev. 27, 1107–1123. https://doi.org/10.1016/j.quascirev.2008.02.009.
Sun, S., Li, M., Yan, M., Fang, X., Zhang, G., Liu, X., Zhang, Z., 2019. Bromine content and Br/Cl molar ratio of halite in a core from Laos: implications for origin and environmental changes. Carbonates Evaporites 34, 1107–1115. https://doi.org/10.1007/s13146-019-00508-0.
Teatini, P., Putti, M., Rorai, C., Mazzia, A., Gambolati, G., Tosi, L., Carbognin, L., 2009. Modeling the saltwater intrusion in the lowlying catchment of the southern Venice Lagoon, Italy. WIT Trans. Ecol. Environ. 127, 351–362. https://doi.org/10.2495/RAV090311.
Teatini, P., Tosi, L., Viezzoli, A., Baradello, L., Zecchin, M., Silvestri, S., 2011. Understanding the hydrogeology of the Venice Lagoon subsurface with airborne electromagnetics. J. Hydrol. 411, 342–3549. https://doi.org/10.1016/j.jhydrol.2011.10.017.
Torresan, S., Critto, A., Rizzi, J., Marcomini, A., 2012. Assessment of coastal vulnerability to climate change hazards at the regional scale: the case study of the North Adriatic Sea. Nat. Hazards Earth Syst. Sci. 12, 2347–2368. https://doi.org/10.5194/nhess-12-2347-2012, 2012.
Tosi, L., Rizzetto, F., Zecchin, M., Brancolini, G., Baradello, L., 2009. Morphostratigraphic framework of the Venice Lagoon (Italy) by very shallow water VHRS surveys: evidence of radical changes triggered by human-induced river diversions. Geophys. Res. Lett. 36 https://doi.org/10.1029/2008GL037136.
Tosi, L., Da Lio, C., Strozzi, T., Teatini, P., 2016. Combining L- and X-Band SAR interferometry to assess ground displacements in heterogeneous coastal

environments: the Po River Delta and Venice Lagoon, Italy. Remote Sens. 8 (4), 308. https://doi.org/10.3390/rs8040308.

Tosi, L., Da Lio, C., Teatini, P., Menghini, A., Viezzoli, A., 2018. Continental and marine surficial water - groundwater interactions: the case of the southern coastland of Venice (Italy). Proc. Int. Assoc. Hydrol. Sci. 379, 387–392. https://doi.org/10.5194/piahs-379-387-2018.

Tosi, L., Da Lio, C., Bergamasco, A., Cosma, M., Cavallina, C., Fasson, A., Viezzoli, A., Zaggia, L., Donnici, S., 2022. Sensitivity, hazard, and vulnerability of farmlands to saltwater intrusion in low-lying coastal areas of Venice, Italy. Water 14 (1), 64. https://doi.org/10.3390/w14010064.

Tran, L.T., Larsen, F., Pham, N.Q., Christiansen, A.V., Tran, N., Vu, H.V., Tran, L.V., Hoang, H.V., Hinsby, K., 2012. Origin and extent of fresh groundwater, salty paleowaters and recent saltwater intrusions in Red River flood plain aquifers, Vietnam. Hydrogeol. J. 20, 1295–1313. https://doi.org/10.1007/s10040-012-0874-y.

Viezzoli, A., Tosi, L., Teatini, P., Silvestri, S., 2010. Surface water-groundwater exchange in transitional coastal environments by airborne electromagnetics: the Venice Lagoon example. Geophys. Res. Lett. 37, L01402 https://doi.org/10.1029/2009GL041572.

Wen, X., Wu, Y., Su, J., Zhang, Y., Liu, F., 2005. Hydrochemical characteristics and salinity of groundwater in the Ejina Basin, Northwestern China. Environ. Geol. 48, 665–675. https://doi.org/10.1007/s00254-005-0001-7.

Werner, A.D., Gallagher, M.R., 2006. Characterisation of sea-water intrusion in the Pioneer Valley, Australia using hydrochemistry and three-dimensional numerical modelling. Hydrogeol. J. 14 (8), 1452–1469. https://doi.org/10.1007/s10040-006-0059-7.

Wu, P., Christidis, N., Stott, P., 2013. Anthropogenic impact on Earth's hydrological cycle. Nat. Clim. Chang. 3 (9), 807–810. https://doi.org/10.1038/nclimate1932.

Zancanaro, E., Teatini, P., Scudiero, E., Morari, F., 2020. Identification of the origins of vadose-zone salinity on an agricultural site in the Venice coastland by ionic molar ratio analysis. Water 12 (12), 3363. https://doi.org/10.3390/w12123363.

Zecchin, M., Brancolini, G., Tosi, L., Rizzetto, F., Caffau, M., Baradello, L., 2009. Anatomy of the Holocene succession of the southern Venice lagoon revealed by very high-resolution seismic data. Cont. Shelf Res. 29, 1343–1359. https://doi.org/10.1016/j.csr.2009.03.006.

Zhang, D., Yan, M., Fang, X., Yang, Y., Zhang, T., Zan, J., Zhang, W., Liu, C., Yang, Q., 2018. Magnetostratigraphic study of the potash-bearing strata from drilling core ZK2893 in the Sakhon Nakhon Basin, eastern Khorat Plateau. Palaeogeogr. Palaeoclimatol. Palaeoecol. 489, 40–51. https://doi.org/10.1016/j.palaeo.2017.08.030.